

**16th  
SYMPOSIUM  
OF THE IAHR**  
SECTION ON HYDRAULIC MACHINERY  
AND CAVITATION  
SAO PAULO / BRAZIL

14<sup>th</sup> to 18<sup>th</sup> SEPTEMBER 1982



## THE IMHEF SYSTEM FOR CAVITATION NUCLEI INJECTION

### L'INJECTEUR DE GERMES DE CAVITATION DE L'IMHEF

Carola BRAND	Ecole Polytechnique Fédérale de Lausanne 33, Avenue de Cour 1007 Lausanne, Switzerland	Switzerland
François AVELLAN	Ecole Polytechnique Fédérale de Lausanne	Switzerland

### SUMMARY

The necessity of controlling the nuclei content of the circuit water while conducting cavitation tests on model hydraulic machines is considered to be indispensable. We are presenting a description of our cavitation nuclei producing device, the so-called nuclei injector, which is based on the principle of rapid expansion of air-saturated water. An experimental study has been carried out on a transparent model injector which has permitted to realize the visualization of the process in the form of photographs or digitized images. This study has allowed the authors to specify the influence of injection parameters (inlet and outlet pressures) on the dimension and the number of cavitation nuclei produced.

### RESUME

La nécessité de contrôler l'état de nucléation de l'eau durant les essais de cavitation des modèles de turbines hydrauliques est désormais bien réelle. Nous présentons une description de notre système d'injection de germes de cavitation, un système dont le principe repose sur une expansion rapide d'eau engazée. Une étude expérimentale a été effectuée sur un modèle transparent de l'injecteur permettant de réaliser des visualisations sous forme de photographies ou d'images digitalisées. Cette étude nous a permis de préciser le rôle des paramètres d'injection (pressions d'entrée et de sortie) sur la dimension et le nombre de noyaux de cavitation produits.

## INTRODUCTION

Cavitation tests on hydraulic machine models have to be carried out with water containing a minimum number of active nuclei in order to allow transposition of the results obtained with the model to the prototype. Beyond this minimum number of active nuclei the model performance is no longer affected by the quantity of active nuclei and the cavitation characteristic is called saturation characteristic [1]. In order to achieve the required nuclei content, micro-bubbles can be seeded into the test rig. One possibility is to create micro-bubbles by a rapid expansion of water saturated with a gas, for example air, through very small orifices [2]. The pressure drop through these orifices leads to a cavity development at the outlet and it results in the formation of micro-bubbles. The IMHEF nuclei injector is based on this technique and has been used in a number of cavitation tests in combination with a Venturi nuclei counter [3]. If much of literature has been dedicated to the nuclei counter techniques [4], there is a lack of published articles on the characteristics of nuclei injectors [5]. For this reason we have carried out a study of our injection system leading to a better understanding of the physical process of the micro-bubble generation. The main aim of this study is to quantify the number of micro-bubbles produced per unit of time and their diameter as a function of operating parameters. This knowledge is necessary in order to carry out a reliable cavitation test. Moreover it is of even greater interest if the International Electrotechnical Commission (IEC) recommends nuclei control in the revised standards of model acceptance tests of hydraulic turbines.

## OPERATING PRINCIPLE OF THE IMHEF NUCLEI INJECTOR

The micro-bubble injection system is composed of two parts, the first consists of the continuous production of air-saturated water and the other one is concerned with the actual generation and injection of cavitation nuclei, Figure 1.

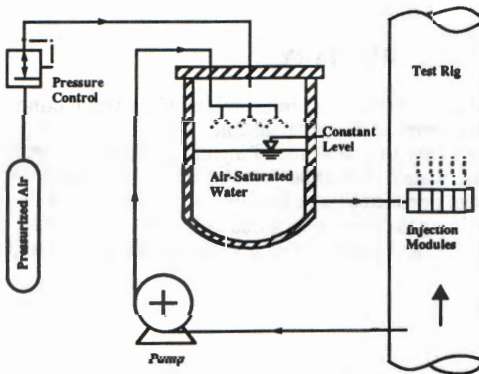


Figure 1 Operation of the IMHEF nuclei-injection system

The saturation of the water with air is obtained by producing a water spray at high pressure, 10 to 30 bar. This is achieved by injecting water through nozzles into a high pressure tank whose volume

is 80 l. The water droplets generated by the nozzles drop to the free surface. The free surface level corresponds approximately to one half of the tank height. A volumetric pump is used to maintain a constant level in the pressure tank which allows a delivery of a steady flow of air-saturated water up to  $1.2 \text{ m}^3\text{h}^{-1}$ . A pressure regulator maintains the pressure difference between the pressure in the tank and the pressure in the test rig. The nuclei are generated by a sudden expansion of the air-saturated water through a series of injection modules. One of these modules consists of two concentric stainless steel discs of 48 mm diameter which are mounted facing each other. The air-saturated water enters a hole of 2 mm diameter in the center of one of the discs, Figure 2. The radial water passage is realized through a groove of 0.1 mm depth and 16 mm width milled on the face of the opposite disc. Each injection module supplies a fixed quantity of cavitation nuclei. By varying the number of injection modules one can obtain the required quantity of cavitation nuclei in the test rig. The maximum flow is  $1.2 \text{ m}^3\text{h}^{-1}$  for 16 injectors and the maximum pressure of the test environment is 16 bar.

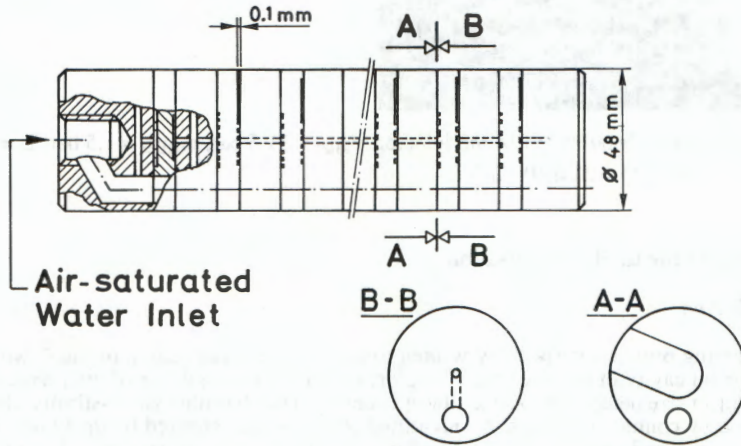


Figure 2 Geometry of an injection module and the assembled structure

## VISUALIZATION EXPERIMENTS

### Visualization of the cavity generation in the injector

In order to visualize the micro-bubbles in the nuclei-injector a transparent model of the injector made by using optical glasses was designed. A Xenon flash lamp and a 35 mm camera with a Micro-Nikkor objective of 55 mm focal length are used to take macrophotographs of the cavity development in the transparent model. A photograph taken under typical conditions of nuclei injection is shown in Figure 3. An attached cavity is observed around the circular line of the outlet of the hole into the passage between the discs. This cavity has the form of an asymmetric crown, corresponding to the asymmetric geometry of the passage. Behind this attached cavity, micro-bubbles can be seen in the flow, on the photograph as small white points of a diameter in the range of  $10 \mu\text{m}$  to  $30 \mu\text{m}$  in full scale. To carry out automatic image treatment on this kind of visualizations, digitized images of the zone downstream the attached cavity are taken with a CCD camera equipped with 500x582 photoelements and a zoom-objective. A Xenon flash lamp synchronized with the camera is used for illumination. A video card of four frame memory buffers

and 256 grey levels is used to capture and process the image. A spatial resolution of 11  $\mu\text{m}$  is achieved in the case of these visualizations .

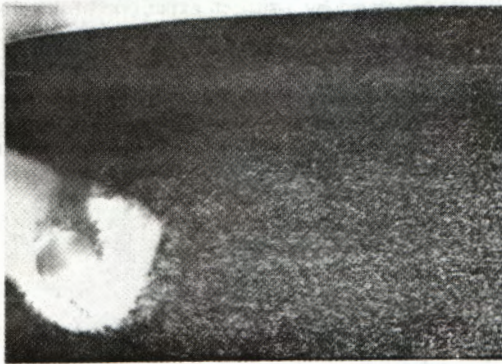


**Figure 3** Cavity visualization in the injector.  $p_{\text{inlet}} = 11.5 \text{ bar}$ ,  $p_{\text{outlet}} = 1.5 \text{ bar}$ ,  $L = 3 \text{ mm}$ ,  $\sigma = 0.2$ ,  $Q = 21.6 \cdot 10^{-6} \text{ m}^3\text{s}^{-1}$ .

### Image processing of the cavity visualization

#### *Aspect ratio criterion*

An image processing program is specially written to analyze the visualization of the downstream zone of the attached cavity in the injector. This program allows thresholding of the image, object identification, object size determination and object counting. The algorithm automatically identifies the object formed by contiguous pixels. An identified object is characterized by its dimensions  $dx$  and  $dy$  in the two perpendicular directions  $x$  and  $y$  of the image. The images are taken in such a way that the  $x$ -direction corresponds to the main flow direction and the  $y$  direction to the direction perpendicular to the main flow. The objects are assumed to be spherical bubbles. Thus owing to the motion of the micro-bubble during the flash duration time, their image has nearly the shape of an ellipse. The small axis  $dy$  of the ellipse corresponds to the diameter  $D$  of a micro-bubble. The large axis of the ellipse corresponds to the sum of the diameter and the displacement of the micro-bubble during the flash duration:

$$dy = D$$

$$dx = D + C \cdot t_{1/\beta}$$

with  $C = 10.5 \text{ ms}^{-1}$  (flow velocity) and  $t_{1/\beta} \approx 0.5 \mu\text{s}$  (flash duration time).

For spatial resolution of the images, the diameter of any object is limited to the minimum diameter  $D_{\text{lim}} = 11 \mu\text{m}$  identifiable by the program. Thus the aspect ratio between  $dx$  and  $dy$  is maximum for the minimum diameter. This relation allows us to build a criterion for the identification of a micro-bubble which corresponds to an aspect ratio smaller than  $f_{\text{max}}$  :

$$\frac{dx}{dy} = \frac{D+X}{D} < f_{\text{max}} = 1.48$$

The discarded objects represent for example amorphous bubble-agglomerations or the images of dust particles on the optical devices.

### Thresholding criterion

Thresholding is a procedure used to distinguish the objects from the background. By thresholding, a zero grey level, which is black, is assigned to all pixels with a grey level lower than the threshold level. To pixels of a grey level equal or higher than the threshold level, a grey level of 255, which is white, is assigned. Thresholding is always a subjective operation and the error made can only be estimated by using a reference measurement method, for example a holographic method. However, if thresholding is carried out in the same way for all the cases treated, we obtain data points that are comparable amongst themselves. As a criteria for threshold choice, we choose the number of micro-bubbles identified for each threshold. When calculating the number of micro-bubbles for all possible thresholds (0 to 255) we find zero objects for the threshold of zero as well as zero objects for the threshold of 255. In between there is a maximum number of objects identified for a certain threshold. This maximum number of identified micro-bubbles is considered as the desired data point. In fact, this method corresponds to a normalization of the images, eliminating the effects of a variation in illumination during the image acquisition.

## EXPERIMENTAL RESULTS

### Main cavity length

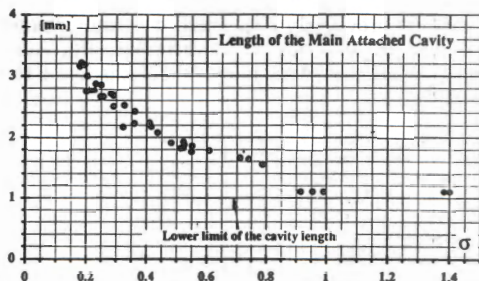


Figure 4 Cavity length of the main cavity as a function of the cavitation coefficient.

By varying both the inlet and the outlet pressure we can perform systematic visualizations of the main cavity development in the injectors. The length  $L$  of the main attached cavity taken in the main flow direction is measured on photographs such as the one shown in Figure 3. The cavitation coefficient  $\sigma$  is defined as follows:

$$\sigma = \frac{p_{\text{outlet}} - p_v}{\rho \frac{C_{\text{ref}}^2}{2}}$$

where  $p_{\text{outlet}}$  is the pressure at the outlet of the injector and  $C_{\text{ref}}$  is the reference velocity defined at the smallest flow section in the injector. The length data can be reduced to a single curve only as a function of the cavitation coefficient, Figure 4. At a value of the cavitation coefficient higher than 1.5, cavitation no longer takes place.

### Concentration of the generated micro-bubbles

Micro-bubble concentration  $C_b$  can also be derived from the above described image treatment. The experimental results are shown in Figure 5. Indeed, the concentration of generated micro-bubbles

is, for a given gas and a given geometry of the saturation system, a unique function of the cavitation coefficient.

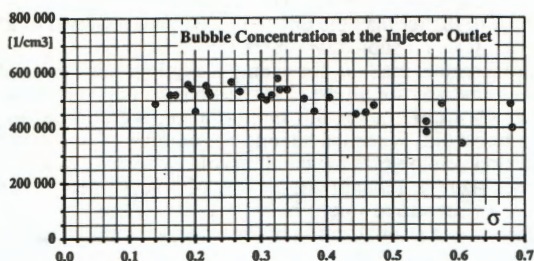


Figure 5 Concentration of the generated micro-bubbles as a function of the cavitation coefficient.

### Diameter of the generated micro-bubbles

By using the image processing method previously described, the mean diameter of the micro-bubbles generated in the injector can be determined for different inlet and outlet pressures. Similarly to the main cavity length, the diameter of the micro-bubbles is found to be simply related to the cavitation coefficient, Figure 6.

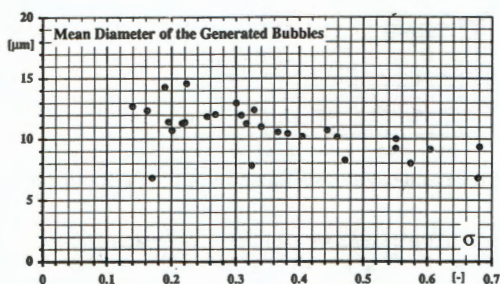


Figure 6 Mean diameter of the generated micro-bubbles as a function of the cavitation coefficient.

## DISCUSSION

### Nuclei concentration

The water used in the injection system contains solid particles, dissolved gas and micro-bubbles of gas as impurities. On the one hand the process of "saturation" with air in the high pressure tank of the system increases the dissolved air-content of the water. On the other hand, micro-bubbles are also added to the water when water droplets fall through the air-chamber of the high-pressure tank. We suppose that the large pressure drop in the injector causes explosion of micro-bubbles that are already present in the water (cavitation) and a transport of gas across the surfaces of exploding micro-bubbles (diffusion). At the same time, a formation of new micro-bubbles due to the supersaturation of the water after the expansion takes place (nucleation). Neglecting the effects of

coalescence of micro-bubbles, the concentration of micro-bubbles can be expressed as the sum of micro-bubbles already existing in the water after the process of saturation in the pressure tank and the additional micro-bubbles generated by nucleation:

$$C_b = C_{b,0} + C_{b,nucl}$$

The original micro-bubble concentration is supposed to be constant for a given water and nozzle geometry. Consequently, for a given geometry and a given gas used, only the contribution of the nucleation is a function of the operating parameters.

When the saturated water is expanded, the water is strongly over-saturated and a certain volume of gas  $\Delta V_{air}$  has to evolve from the solution in order to reach equilibrium for the new pressure. We suppose that this volume of potentially evolving gas represents the driving force for the nucleation.

$$C_{b,nucl} = f(\Delta V_{air})$$

By using Henry's Law for the inlet and the outlet of the injector we can calculate  $\Delta V_{air}$  for our data points:

$$\frac{\Delta V_{air}}{V_{water}} = \frac{P_{inlet} - P_{outlet}}{H} \frac{M_{air}}{M_{water}} \frac{\rho_{water}}{\rho_{air}}$$

The plot of the measured micro-bubble concentrations versus the ratio  $\frac{\Delta V_{air}}{V_{water}}$  confirms our assumption, Figure 7.

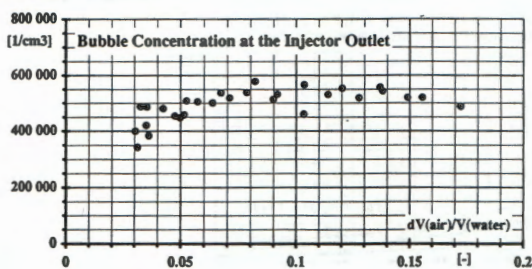


Figure 7 Micro-bubble concentration as a function of  $\frac{\Delta V_{air}}{V_{water}}$ .

The volume  $\Delta V_{air}$  is the maximum air volume that can evolve from the solution by the expansion calculated for the outlet pressure. This volume is a theoretical value and can not be simply used to calculate a micro-bubble volume or a micro-bubble concentration, because any micro-bubbles generated in the injector will contain a mixture of gas and vapor, leading to a density which depends on the ratio of gas and vapor volume in the micro-bubbles. By supposing that the gas behaves like a perfect gas the density of the air at the outlet condition is:

$$\rho_{air} = \frac{M_{air} P_{outlet}}{R T}$$

we can write:

$$\left(\frac{\Delta V_{\text{air}}}{V_{\text{water}}}\right) \sim \left(\frac{\Delta P}{P_{\text{outlet}}}\right)$$

If we formulate the flow rate in the injector by

$$Q^2 = K \Delta P$$

the cavitation coefficient becomes:

$$\sigma = \frac{P_{\text{outlet}} - P_{\text{vapour}}}{\frac{1}{2} \rho \frac{K \Delta P}{A_{\text{ref}}^2}}$$

and it results:

$$\left(\frac{\Delta V_{\text{air}}}{V_{\text{water}}}\right) \sim \frac{1}{\sigma}$$

The above deduction is only a qualitative consideration. However, it gives us a better understanding why the concentration of generated micro-bubbles is a unique function of the cavitation coefficient, as it has been obvious from the experiments. For the operation of the injector, this result is extremely useful and it can be transformed directly into operation curves. Thus, the micro-bubble concentration in the test rig at a given injection condition can be determined, Figure 8.

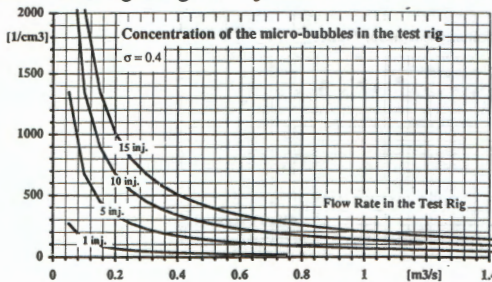


Figure 8 Micro-bubble concentration in the test rig for different numbers of injector modules calculated for a cavitation coefficient in the injector of  $\sigma=0.4$ .

#### Diameter of the generated micro-bubbles

We have seen that for a given injector geometry, the final mean size of the cavitation nuclei is driven by the value of the cavitation coefficient. To overcome the influence of the actual pressure we can compute an equivalent diameter  $D_0$  related to a given reference pressure  $p_0$  for all data points. If we assume an adiabatic volume change of the micro-bubbles, the diameter  $D_0$  of a micro-bubble at a reference pressure  $p_0$  can be calculated from the actual diameter  $D$  and the actual pressure  $p$  as follows:

$$\frac{D_0}{D} = \left[\frac{p}{p_0}\right]^{\frac{1}{3\Gamma}}$$



where  $\Gamma$  is the ratio of specific heats,  $c_p/c_v = 1.4$  for air. When plotting  $D_0$  versus the cavitation coefficient the result is that the reference diameter  $D_0$  does not vary with the cavitation coefficient, Figure 9. This means that the mean mass of gas contained in the micro-bubbles is constant for different values of the cavitation coefficient. Consequently we can state that the length of the cavity does not play an important role for the final micro-bubble diameter.

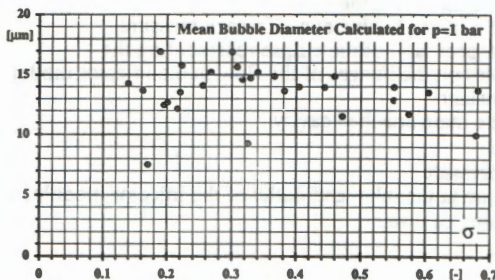


Figure 9 Mean micro-bubble diameter calculated for the reference pressure  $p_0=1$  bar.

The fact that the mass of gas contained in the micro-bubbles is independent of the cavitation coefficient, allows us to calculate the mean diameter of the generated micro-bubbles for different injector outlet pressures, using the equation above. The plot of the mean diameter versus the injector outlet pressure is finally a directly applicable operation curve, Figure 10.

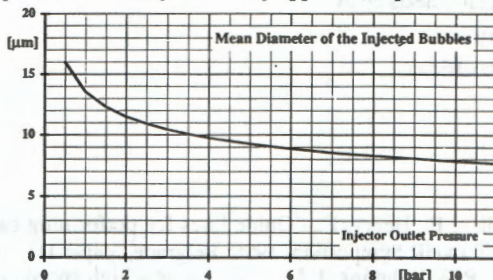


Figure 10 Mean diameter of the micro-bubbles versus the injector outlet pressure.

## CONCLUSIONS

The results of the study on IMHEF micro-bubble injection system allow us to predict the dimension and the concentration of the micro-bubbles generated by the system knowing the injection operating conditions. The development of a cavity in the nuclei injectors leads to a proper operation of the system. The mean diameter of the generated micro-bubbles depends only on the injector outlet pressure which corresponds to the actual test rig pressure. In the pressure range of 0.5 bar to 11 bar the mean diameter lies between 16  $\mu\text{m}$  and 9  $\mu\text{m}$ . Furthermore, the concentration of the injected micro-bubbles depends on the cavitation coefficient, formulated for the injector. But, the dependence is weak and a concentration of 500 000 nuclei/ $\text{cm}^3$  at the injector outlet is a good mean value for the used range of the injector cavitation coefficient. However, the determination of the number of injector modules necessary to achieve a required cavitation nuclei concentration in the test rig is then possible by the use of the results of our study. This is of a great importance in order to achieve reliable cavitation tests of modern hydraulic units.

## LIST OF SYMBOLS

$C_b$	Concentration of micro-bubbles per unit of volume	$\text{cm}^{-3}$
$C_{ref}$	Reference velocity	$\text{m s}^{-1}$
$D$	Diameter of a micro-bubble	$\text{m}$
$D_0$	Diameter of a micro-bubble at a reference pressure	$\text{m}$
$f_{max}$	Maximum aspect ratio of the ellipse representing the micro-bubbles on the images of the flow in the injector model	
$H$	Henry's constant	$\text{Pa}$
$L$	Length of the main attached cavity	$\text{m}$
$M$	Molar mass	$\text{kg mol}^{-1}$
$p_0$	Reference pressure	$\text{Pa}$
$p_{inlet}, p_{outlet}$	Static pressure at the inlet and outlet of the injector module	$\text{Pa}$
$p_v$	Vapor pressure of water	$\text{Pa}$
$\Delta p$	$p_{inlet} - p_{outlet}$	$\text{Pa}$
$Q$	Flow rate	$\text{m}^3 \text{s}^{-1}$
$R$	General gas constant	$\text{J mol}^{-1} \text{K}^{-1}$
$T$	Temperature	$\text{K}$
$V_{water}$	Water volume	$\text{m}^3$
$\Delta V_{air}$	Theoretical maximum air volume evolving from the water after the expansion, calculated for the outlet pressure	$\text{m}^3$
$\Gamma$	Ratio of specific heats $c_p/c_v$	
$\rho$	Mass density	$\text{kg m}^{-3}$
$\sigma$	Cavitation coefficient	

## REFERENCES

- [1] Gindroz, B., Avellan, F., Henry, P., "Guide lines for performing cavitation tests", Proceedings of 15<sup>th</sup> IAHR Symposium, 1990, Belgrade, paper H1, pp 1-11.
- [2] Avellan, F., Henry, P. & Ryhming, I. L., 1987, "A new high speed cavitation tunnel for cavitation studies in hydraulic machinery", Proc. of International Symposium on Cavitation Research Facilities and Techniques, ASME Winter Annual Meeting, Boston (USA), FED: Vol. 57, Dec 1987, pp 49-60.
- [3] Gindroz, B., Avellan, F., Henry, P., "Similarity Rules of Cavitation Tests : the Case of Francis Turbine", Proceedings of 14<sup>th</sup> IAHR Symposium on Hydraulic Machinery : Progress within Large and High Specific Energy Units, 1988, Trondheim, pp 755-756.
- [4] Gindroz, B. "Comparaison expérimentale de technique de mesure de germes de cavitation", 2<sup>ème</sup> journées Cavitation, Colloque d'Hydrotechnique, Session N°144 Société Hydrotechnique de France, mars 1992, Paris.
- [5] Lecoffre, Y., Marcoz, J., Valibouse, B., "Aspects pratiques du contrôle de germes de cavitation en moyens d'essais", *Proceedings of AIRH Symposium on operating problems of pump stations and power plants*, 1982, Amsterdam, pp. 7.1-7.15.